$Bi_{1-x}Sr_xCuSeO$ oxyselenides as promising thermoelectric materials

L. D. Zhao,[1,2,a] D. Berardan,[1,2] Y. L. Pei,[3] C. Byl,[1,2] L. Pinsard-Gaudart,[1,2] and N. Dragoe[1,2]

[1]*Institut de Chimie Moléculaire et des Matériaux d'Orsay, Univ. Paris-Sud, UMR 8182, Orsay F-91405, France*

[2]*CNRS, Orsay F-91405, France*

[3]*School of Materials Science and Engineering, Beihang University, Beijing 100191, People's Republic of China*

(Received 4 July 2010; accepted 11 August 2010; published online 3 September 2010)

p-type BiCuSeO, a layered oxyselenide composed of conductive $(Cu_2Se_2)^{2-}$ layers alternately stacked with insulating $(Bi_2O_2)^{2+}$ layers, shows an enhancement of the electrical conductivity after substituting Bi^{3+} by Sr^{2+}, from 470 S m^{-1} (BiCuSeO) to 4.8×10^4 S m^{-1} ($Bi_{0.85}Sr_{0.15}CuSeO$) at 293 K. Coupled to high Seebeck coefficients, this leads to promising values of the thermoelectric power factor that exceeds 500 μW m^{-1} K^{-2} at 873 K. Moreover, the thermal conductivity of these layered compounds is lower than 1 W m^{-1} K^{-1} at 873 K. Maximum *ZT* values reach 0.76 at 873 K, making this family promising for thermoelectric applications in the medium temperature range. [doi:10.1063/1.3485050]

Thermoelectric (TE) materials are receiving increasing attention because of their possible applications in power generation and electronic cooling. The efficiency of TE devices is determined by the dimensionless figure of merit (*ZT*), defined as $ZT=(\alpha^2\sigma/k)T$, where α, σ, k, and T are the Seebeck coefficient, the electrical conductivity, the thermal conductivity, and the absolute temperature, respectively.[1] Up to now, several classes of bulk materials with high *ZT* values have been discovered,[2] including nanostructured BiSbTe alloys, filled skutterudites, zinc antimonide, $AgPb_{18+x}SbTe_{20}$, Tl doped PbTe, and $(AgSbTe_2)_{1-x}(GeTe)_x$ alloys. Besides these materials, many compounds were reported as promising TE materials, including Ag_9TlTe_5, In_4Se_3, and In_4Te_3 and Cu_2ZnSnQ_4 (Q=S, Se).[3,4] Among them, the case of Cu_2ZnSnQ_4 (Q=S, Se) compounds is interesting. It is usually accepted that good TE materials should be narrow-band-gap semiconductors. However, $Cu_2ZnSnSe_4$ based compounds with a wide band gap of 1.44 eV also exhibits high *ZT* values, reaching 0.91 at 860 K for $Cu_{2.1}Zn_{0.9}SnSe_4$[3] and 0.95 at 850 K for $Cu_2ZnSn_{0.9}In_{0.1}Se_4$.[4] Some wide-band-gap oxides also exhibit promising TE properties, with $ZT=0.65$ at 1247 K in $Zn_{0.96}Al_{0.02}Ga_{0.02}O$ (3.3 eV)[5] or $ZT=0.45$ at 1273 K in $In_{1.8}Ge_{0.2}O_3$ (3.6 eV).[6] These results open a way for exploring high-performance TE materials within the family of wide-band-gap semiconductors. Following this concept, this paper focuses on the quaternary oxyselenide BiCuSeO, with a band gap of 0.8 eV.[7]

Samples with the chemical composition $Bi_{1-x}Sr_xCuSeO$ (x=0, 0.025, 0.05, 0.075, 0.10, 0.125, and 0.15) were synthesized using a two-step solid state reaction route similarly to a previous report.[7] The obtained samples were ground and subsequently densified by using a spark plasma sintering (SPS) system (SPS-511S) at 973 K with holding time of 7 min in a Φ 12 mm graphite die under an axial compressive stress of 60 MPa in an argon atmosphere. X-ray diffraction characterization was performed using a Panalytical X'Pert diffractometer with a Ge (111) incident monochromator and an X'celerator detector. Rietveld refinement was performed using FULLPROF software.[8] Electrical resistivity and Seebeck coefficient were measured simultaneously by the standard four-probe method using a laboratory made system in argon atmosphere. The thermal diffusivity coefficient λ was determined using a laser flash method (Netzsch LFA 427). The thermal conductivity was calculated from $k=\lambda\ C_p d$, where C_p is the specific heat capacity (NETZSCH, STA 429) and d is the density (measured using Archimedes method). The measured relative densities of all the samples are about 97%. It should be noted that differential scanning calorimetry (DSC) results indicate that $Bi_{1-x}Sr_xCuSeO$ samples are stable up to 973 K. Therefore, all transport measurements were performed in the temperature range from 293 to 873 K.

Figure 1(a) shows the BiCuSeO crystal structure, which belongs to the ZrSiCuAs structure type in the tetragonal $P4/mm$ space group. This composite crystal structure is constituted by $(Cu_2Se_2)^{2-}$ layers alternately stacked with $(Bi_2O_2)^{2+}$ layers along the c axis of the tetragonal cell. Figure 1(b) shows the diffraction pattern and Rietveld refinement of SPSed $Bi_{0.975}Sr_{0.025}CuSeO$. The agreement between the experimental data (red circle) and the calculations (black line) is good and the R_{wp} (weighted residual error, blue line) factor is about 11.7%, the others typical R values for all refinements are $R_p\sim8.9\%$ and $R_{Bragg}\sim2.5\%$. Figure 1(c) shows the XRD patterns of SPSed $Bi_{1-x}Sr_xCuSeO$ (x =0–0.15). All major Bragg peaks can be indexed in the ZrSiCuAs structure type. At high Sr content, Sr>0.1, a splitting of the Bragg peaks can be observed (see for example at $2\theta=53°$). Both phases can be indexed in the ZrSiCuAs structure type with distinct sets of lattice parameters, for example a=3.930 Å and c=8.927 Å, and a=3.942 Å and c =9.036 Å for a nominal composition of Sr=0.15. This result is consistent with EDX measurements that evidence the presence of two mean compositions, one with low Sr content and one with higher Sr content. It could be linked to the presence of an immiscibility gap or an incomplete diffusion of strontium and bismuth in the samples. However, no other Bragg

[a]Author to whom correspondence should be addressed. Electronic mail: lidong.zhao@u-psud.fr.

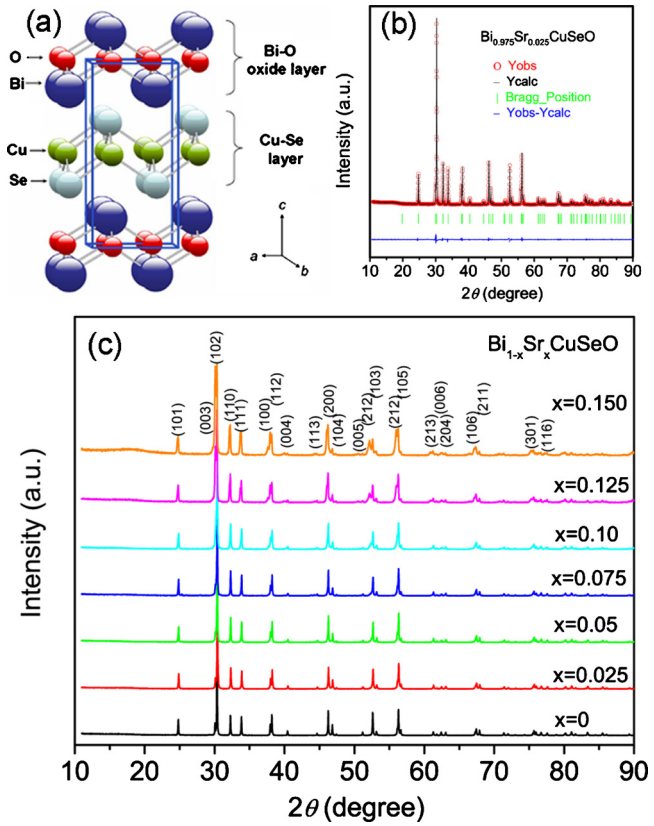

FIG. 1. (Color online) (a) Crystal structure for BiCuSeO of ZrSiCuAs structure type in the tetragonal $P4/nnm$ space group (No.129), the solid-line box shows a unit cell, (b) XRD pattern and Rietveld refinement of SPSed $Bi_{0.975}Sr_{0.025}CuSeO$, and (c) Powders XRD patterns of SPSed $Bi_{1-x}Sr_xCuSeO$.

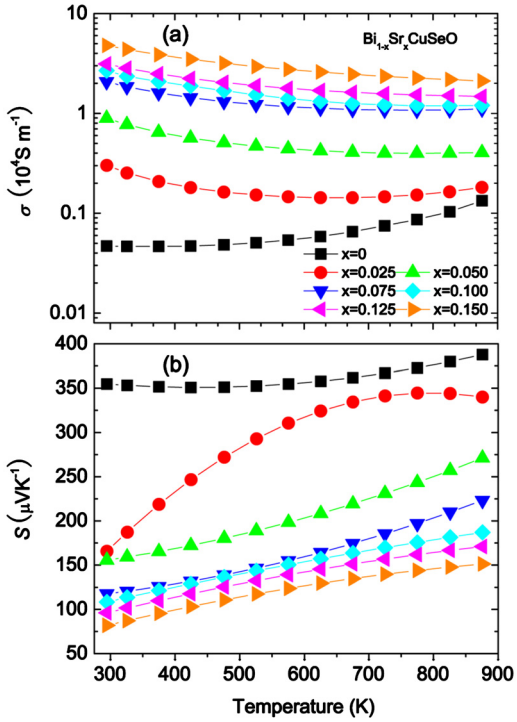

FIG. 2. (Color online) Temperature dependence of electrical transport properties of $Bi_{1-x}Sr_xCuSeO$: (a) electrical conductivity, (b) Seebeck coefficient.

peaks can be detected outside the 1111 phases. Therefore, the samples with high Sr contents can be considered as composites samples, with the nominal Sr compositions corresponding to a mean composition. However, this does not call into question the main results of this paper regarding TE properties. BiCuSeO crystallizes in a layered structure, and could therefore exhibit preferential orientation following the uniaxial densification process. However, the XRD patterns for $Bi_{1-x}Sr_xCuSeO$ samples along the sections perpendicular and parallel to the SPS pressing direction do not evidence any preferential orientation of the crystallites. Therefore, the TE transport properties for $Bi_{1-x}Sr_xCuSeO$ polycrystals prepared by SPS with ground powders are assumed to be isotropic.

BiCuSeO exhibits low electrical conductivity values over the whole temperature range, as shown in Fig. 2(a). Electrical transport changes from a semiconductive to a metallic behavior with Sr doping, and the electrical conductivity is significantly enhanced and increases with increasing Sr content, from 470 S m^{-1} (BiCuSeO) to 4.8×10^4 S m^{-1} ($Bi_{0.85}Sr_{0.15}CuSeO$) at 293 K. The electrical conductivity of $Bi_{1-x}Sr_xCuSeO$ is higher than that of $Cu_2ZnSn_{0.85}In_{0.15}Se_4$,[4] and is comparable to that of high-performance BiSbTe.[9] This result indicates that Sr doping can effectively strongly enhance the electrical conductivity of BiCuSeO. This behavior can be easily explained if we consider the iron-based LaFeAsO superconductor.[10] In these materials, that crystallize in the same structure type, the superconductivity can be obtained by electron doping in insulating $(La_2O_2)^{2+}$ layers through partial substitution of O^{2-} by F^-. These $(La_2O_2)^{2+}$ layers act as a charge reservoir that transfers electrons to the $(Fe_2As_2)^{2-}$ layers, while the $(Fe_2As_2)^{2-}$ layers act as conductive layers which are responsible for superconductivity. Similarly, BiCuSeO materials consist in an insulating oxide $(Bi_2O_2)^{2+}$ layer with ionic bonds, that acts as charge reservoir, and a conductive selenide $(Cu_2Se_2)^{2-}$ layer with covalent bonds, that constitutes the conduction pathway for carriers transport. Therefore, enhanced electrical conductivity of $Bi_{1-x}Sr_xCuSeO$ originates from carriers that are induced in the charge reservoir insulating $(Bi_2O_2)^{2+}$ layers through partial substitution of Bi^{3+} by Sr^{2+}, and then transferred to the conductive $(Cu_2Se_2)^{2-}$ layers.

Figure 2(b) shows the temperature dependence of the Seebeck coefficients of $Bi_{1-x}Sr_xCuSeO$. The positive values indicate that electrical transport properties are dominated by holes. The Seebeck coefficient for BiCuSeO is very large, 350 μV/K at 293 K, which is consistent with the low electrical conductivity. It decreases with increasing Sr doping contents over the whole temperature range, down to 82 μV/K for $Bi_{0.85}Sr_{0.15}CuSeO$ at 293 K. All the values of the Seebeck coefficient for Sr doped BiCuSeO samples vary around 82–250 μV/K over the whole temperature range. These values are comparable to those of Cu_2ZnSnQ_4 (Q=S, Se),[3] $Cu_2ZnSn_{1-x}In_xSe_4$ [4] and high-performance $In_xCe_yCo_4Sb_{12}$.[11] Wide-band-gap compounds often show large Seebeck coefficient since wide band gap can suppress the bipolar behavior, usually observed in narrow-band-gap materials. However, these materials are usually characterized by low electrical conductivity.[12] The promising electrical transport behavior (high electrical conductivity coupled to high Seebeck coefficient) for $Bi_{1-x}Sr_xCuSeO$ might be related to its layered crystal structure, with the insulating $(Bi_2O_2)^{2+}$ layers and the conductive $(Cu_2Se_2)^{2-}$ layers forming a natural superlattice, with a two-dimensional (2D) confinement of the charge carriers. Indeed, the natural layered

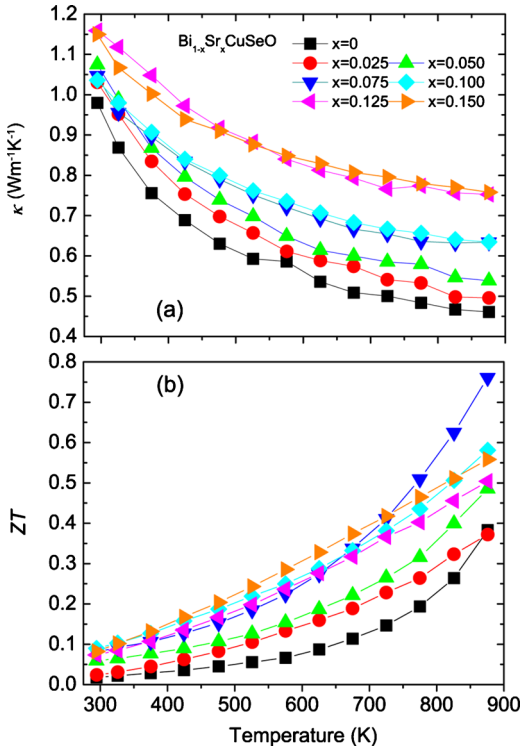

FIG. 3. (Color online) Temperature dependence of (a) thermal conductivity and (b) dimensionless figure of merit *ZT* for $Bi_{1-x}Sr_xCuSeO$.

structure of $(Bi_2O_2)^{2+}/(Cu_2Se_2)^{2-}/(Bi_2O_2)^{2+}$ is very similar to artificial $SrTiO_3/SrTi_{0.8}Nb_{0.2}O_3/SrTiO_3$ (insulating/conductive/insulating) layered structure, which exhibits huge Seebeck coefficient.[13] It has been reported that carriers confined within superlattices[14,15] can yield unusually large Seebeck coefficient without degradation of the other TE values. Indeed, some compounds with natural layered structure show large Seebeck coefficient, including for example iron-based *Ln*FeAsO (*Ln*=La, Sm, and Nd),[16] $Ca_2Co_2O_5$,[17] or La_2CuO_4.[18] In the current materials, good electrical conductivity of BiCuSeO may be realized by doping Sr^{2+} on Bi^{3+} site while keeping a large Seebeck coefficient due to 2D confinement in $(Cu_2Se_2)^{2-}$ layers. The enhanced electrical conductivity and the mostly positive temperature dependence of the Seebeck coefficient cause the power factor ($PF=\alpha^2\sigma$) to increase especially at high temperature, resulting in 500 and 580 $\mu W\,m^{-1}\,K^{-2}$ at 873 K for $Bi_{0.85}Sr_{0.15}CuSeO$ and $Bi_{0.90}Sr_{0.10}CuSeO$, respectively.

Figure 3(a) shows the thermal conductivity values for $Bi_{1-x}Sr_xCuSeO$. The thermal conductivity of undoped BiCuSeO decreases with increasing temperature, from 0.98 $W\,m^{-1}\,K^{-1}$ at 293 K to 0.46 $W\,m^{-1}\,K^{-1}$ at 873 K. This rapid decrease with the temperature indicates that the phonon contribution to the conductivity is predominant. These values are all very low, and comparable to those of high-performance TE materials,[1,2] even lower than that of Bi_2Te_3.[19] The total thermal conductivity is the sum of electronic and lattice contributions. Using the measured electrical conductivity in conjunction with the Wiedemann–Franz law, we can estimate that the maximum thermal conductivity originating from the electrons could be below 0.35% of the total thermal conductivity for the undoped BiCuSeO sample. The low thermal conductivity of $Bi_{1-x}Sr_xCuSeO$ may originate from the layered structure since phonons can be scattered at the layers interfaces,[14,15] from the weak bonding between layers,[2,9,19] from the presence of low-phonon-conductive heavy elements or from some other reasons. This is an open issue yet and needs further clarification. Benefiting from low thermal conductivity, *ZT* is maximum at high temperature, as shown in Fig. 3(b). *ZT* values reach 0.56 and 0.58 at 873 K for $Bi_{0.85}Sr_{0.15}CuSeO$ and $Bi_{0.90}Sr_{0.10}CuSeO$, respectively, and $Bi_{0.925}Sr_{0.075}CuSeO$ exhibits the highest *ZT* values with 0.76 at 873 K. Present work indicates that the TE properties of BiCuSeO have been improved by Sr doping in the insulating $(Bi_2O_2)^{2+}$ layers. It would be interesting to determine whether such an improvement in also possible by introducing holes through direct substitutions in the conductive $(Cu_2Se_2)^{2-}$ layers.

In summary, *p*-type BiCuSeO oxyselenides with a band gap of 0.8 eV evidence excellent electrical conductivity while keeping high Seebeck coefficient after Sr doping on Bi site. The very low thermal conductivity contributes to high *ZT* values that reach 0.76 at 873 K for $Bi_{0.925}Sr_{0.075}CuSeO$. Therefore, BiCuSeO based materials are very promising for applications in TE energy converters in a medium temperature range.

This work was supported by the Triangle de la Physique under Project No. STP 2008-095T and International Cooperation Department of Université Paris-Sud XI.

[1] G. J. Snyder and E. S. Toberer, Nature Mater. **7**, 105 (2008).
[2] A. J. Minnich, M. S.Dresselhaus, Z. F. Ren, and G. Chen, Energy Environ. Sci. **2**, 466 (2009).
[3] M. L. Liu, F. Q. Huang, L. D. Chen, and I. W. Chen, Appl. Phys. Lett. **94**, 202103 (2009).
[4] X. Y. Shi, F. Q. Huang, M. L. Liu, and L. D. Chen, Appl. Phys. Lett. **94**, 122103 (2009).
[5] M. Ohtaki, K. Araki, and K. Yamamoto, J. Electron. Mater. **38**, 1234 (2009).
[6] D. Berardan, E. Guilmeau, A. Maignan, and B. Raveau, Solid State Commun. **146**, 97 (2008).
[7] H. Hiramatsu, H. Yanagi, T. Kamiya, K. Ueda, M. Hirano, and H. Hosono, Chem. Mater. **20**, 326 (2008).
[8] J. Rodriguez-Carvajal, Physica B **192**, 55 (1993).
[9] W. J. Xie, X. F. Tang, Y. G. Yan, Q. J. Zhang, and T. M. Tritt, Appl. Phys. Lett. **94**, 102111 (2009).
[10] Y. Kamihara, H. Hiramatsu, M. Hirano, R. Kawamura, H. Yanagi, T. Kamiya, and H. Hosono, J. Am. Chem. Soc. **130**, 3296 (2008).
[11] H. Li, X. F. Tang, Q. J. Zhang, and C. Uher, Appl. Phys. Lett. **94**, 102114 (2009).
[12] L. D. Zhao, B. P. Zhang, W. S. Liu, H. L. Zhang, and J. F. Li, J. Solid State Chem. **181**, 3278 (2008).
[13] H. Ohta, S. Kim, Y. Mune, T. Mizoguchi, K. Nomura, S. Ohta, T. Nomura, Y. Nakanishi, Y. Ikuhara, M. Hirano, H. Hosono, and K. Koumoto, Nature Mater. **6**, 129 (2007).
[14] R. Venkatasubramanian, E. Siivola, T. Colpitts, and B. O'Quinn, Nature (London) **413**, 597 (2001).
[15] L. D. Hicks and M. S. Dresselhaus, Phys. Rev. B **47**, 12727 (1993).
[16] L. Pinsard-Gaudart, D. Berardan, J. Bobroff, and N. Dragoe, Phys. Status Solidi (RRL) **2**, 185 (2008).
[17] J. L. Lan, Y. H. Lin, G. J. Li, S. L. Xu, Y. Liu, C. W. Nan, and S. J. Zhao, Appl. Phys. Lett. **96**, 192104 (2010).
[18] Y. Liu, Y. H. Lin, B. P. Zhang, H. M. Zhu, C. W. Nan, J. L. Lan, and J. F. Li, J. Am. Ceram. Soc. **92**, 934 (2009).
[19] X. B. Zhao, X. H. Ji, Y. H. Zhang, T. J. Zhu, J. P. Tu, and X. B. Zhang, Appl. Phys. Lett. **86**, 062111 (2005).